

Production of a highly porous material by liquid phase sintering of short ferritic stainless steel fibres and a preliminary study of its mechanical behaviour

A.E. Markaki*, V. Gergely, A. Cockburn, T.W. Clyne

Department of Materials Science & Metallurgy, Cambridge University, Pembroke Street, Cambridge CB2 3QZ, UK

Received 15 March 2003; accepted 5 May 2003

Abstract

A procedure is outlined for the production of highly porous material by liquid phase sintering of short stainless steel fibres, about 100 μm in diameter. The fibres, which were produced by a melt extraction route, were first electroplated with copper to a thickness of a few μm . The sintering procedure was then completed by holding at about 1100 $^{\circ}\text{C}$ for a few minutes. It is shown that this operation generates strong joints by the migration of liquid copper to the fibre–fibre contact regions, as a result of capillary action. A preliminary study of the mechanical behaviour material produced in this way indicates that its toughness is relatively high, for a highly porous metallic material, and that its fracture energy is broadly consistent with predictions from a model based on evaluation of the work done by plastic deformation and rupture of individual fibres close to the fracture plane.

© 2003 Elsevier Ltd. All rights reserved.

1. Introduction

Interest in highly porous metallic materials is currently high and various applications are being explored [1,2]. Unfortunately, the mechanical properties [1,3] of such materials are in many cases very poor, particularly under tensile loading. This is partly due to unavoidable stress localization effects, but these are often exacerbated by severe inhomogeneities and gross defects and by the presence of embrittling constituents in the cell walls [4] (sometimes introduced deliberately to facilitate processing). However, the development of highly porous structures with good mechanical properties should be possible, provided that suitable processing procedures are employed.

Furthermore, there should be scope for tailoring components to the requirements of particular applications, for example by the introduction of porosity gradients or microstructural anisotropy. A promising approach to the generation of highly porous and permeable metallic material with relatively high strength, and with potential scope for flexible tailoring of microstructure and properties, is to strongly bond

together an assembly of fibres or wires. In general, metallic wires are readily available with good mechanical properties. Furthermore, in many cases they can readily be joined, for example by sintering, diffusion bonding or welding. There has been some work on material produced in this way—for example, Ducheyne et al. [5,6] produced material with porosity levels between 30 and 60% by sintering austenitic stainless steel wires, under compression. There are, however, very few reported studies of highly porous (~ 80 – 95% porosity) material being made in this way and, while some work has been done [7,8] on the elastic properties of such material, there is in general little or no information available about strength levels or other mechanical characteristics of such material.

A number of potential applications can be envisaged for highly porous metallic materials with good mechanical properties, including their use in the core of sandwich sheet material [9,10]. In the present paper, a novel method [11] of electroplating short, magnetic fibres is presented. A coating deposited in this way has been found to allow rapid sintering of an array of short fibres into a relatively strong, tough material with high porosity and permeability. Information is given concerning the microstructure of this material and results are presented from a preliminary study of its mechanical properties.

* Corresponding author.

E-mail address: am253@cam.ac.uk (A.E. Markaki).

URL: <http://www.msm.cam.ac.uk>.

2. Experimental procedures

2.1. Material production

Fibres of 446 stainless steel (a ferritic steel with a composition of Fe-26 wt.%Cr-0.12 wt.%C) were melt extracted to lengths of 2.5 mm, at Fibretech Ltd. Continuous fibres were also produced. The morphology and sectional shape of these fibres are illustrated in Fig. 1. The average diameter of the short fibres is about 100 μm , although it can be seen in Fig. 1(b) that the section shape is far from circular. The long fibres also had an average diameter of about 100 μm , but their sectional shape was closer to being circular [Fig. 1(d)]. Furthermore, it can be seen in Fig. 1(a) and (c) that the sectional area of these fibres varies along the length.

A copper coating was deposited onto the short fibres, using the plating bath design shown in Fig. 2. The aqueous electrolyte contained 200 g l⁻¹ of hydrated CuSO₄ and 25 ml l⁻¹ of H₂SO₄. The coating current used was about 1 A, which, for typical fibre loadings, corresponds to a current density of about 10⁻³ A m⁻², generating a copper deposition rate of about 0.04 $\mu\text{m s}^{-1}$. The plating operation thus took about 2 min to generate a 5 μm coating. The fibres were held apart from each other, and were thus uniformly exposed to the electrolyte, using the magnetic support system [11] depicted in the figure. The fibres line up along the lines of magnetic flux. This method is thus applicable to short fibres of any magnetic material. A coated fibre is shown in Fig. 3. (Note that the fibre is only partially coated, but this was found sufficient to create strong joints between adjacent

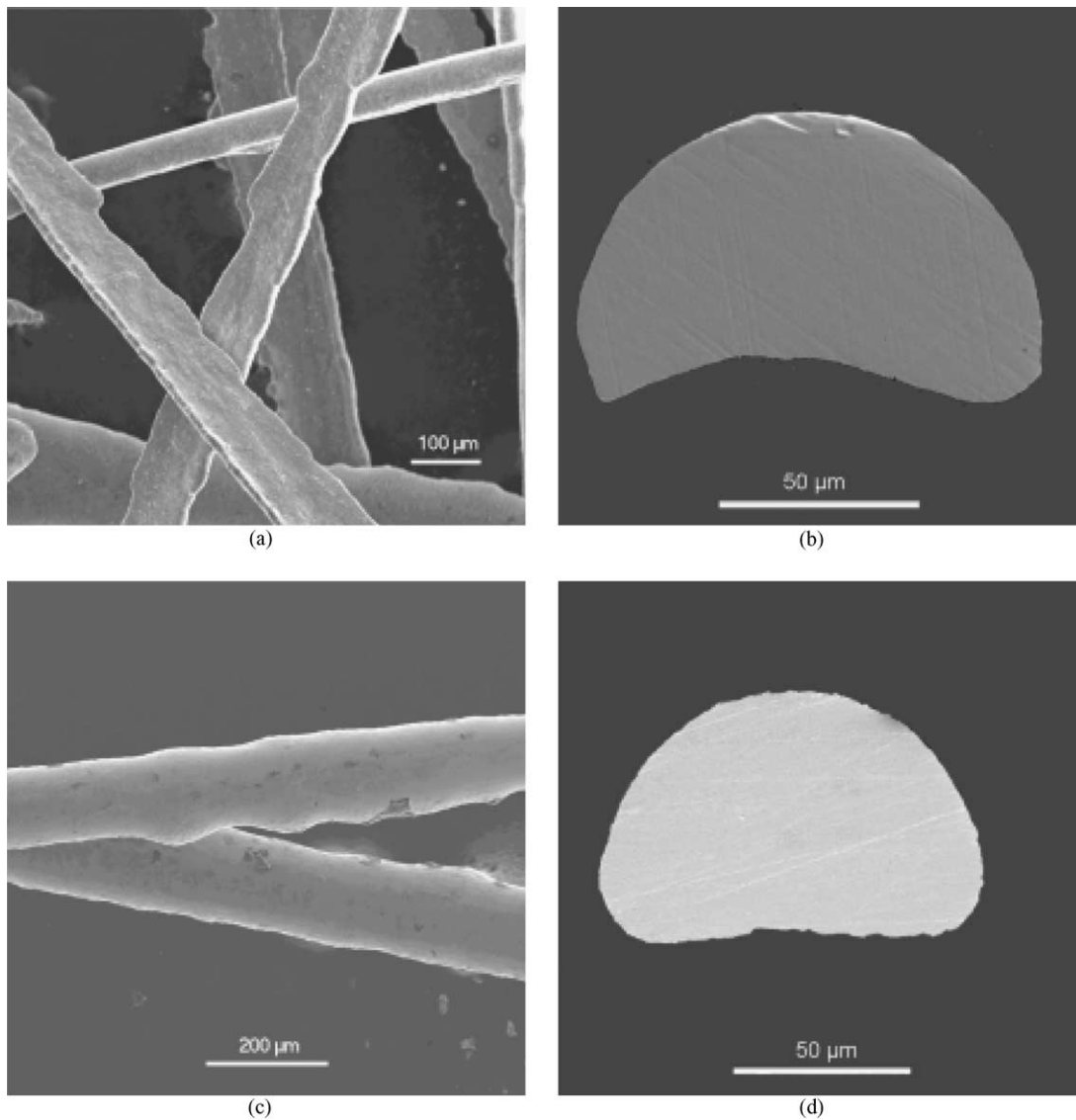


Fig. 1. Scanning electron micrographs showing (a) the overall morphology and (b) the cross-sectional shape of short (2.5 mm long), melt-spun 446 fibres. (c) and (d) are corresponding images for continuous fibres produced in a similar manner.

fibres—see below.) Some of the long fibres were also coated, using similar deposition conditions.

Short coated fibres were packed into a quartz ampoule with a bore of 5 mm, to a length of about 30 mm, so that they occupied a volume fraction of about 10%. (This figure was obtained by simply weighing the fibres, taking account of the fact that they had a 5 μm copper coating.) The ampoule was then evacuated, back-filled with argon and sealed. A thermocouple was attached to the ampoule, close to the fibres, and the assembly was inserted for a short period into a furnace held at 1100 $^{\circ}\text{C}$. A typical thermal history recorded from the thermocouple is shown in Fig. 4. It can be seen that the specimen was exposed to a temperature of about 1100 $^{\circ}\text{C}$, for a period of about 5 min. Since this is above the melting temperature of copper (~ 1083 $^{\circ}\text{C}$), the Cu coating became liquid and was driven by capillary action towards the junctions between the fibres. This process was sufficiently fast to ensure preferential localisation of much of the copper at the fibre joints, before solidification occurred. This can be seen in the SEM micrographs shown in Fig. 5.

2.2. Single fibre tensile testing

The long fibres were subjected to single fibre tensile testing, using a Schenk desktop testing machine, fitted

with a 250 N load cell. Individual fibres were cut to lengths of about 50 mm and were mounted on paper tabs, with a central cut-out that gave a gauge length of about 25 mm. The tab was gripped in the jaws of the

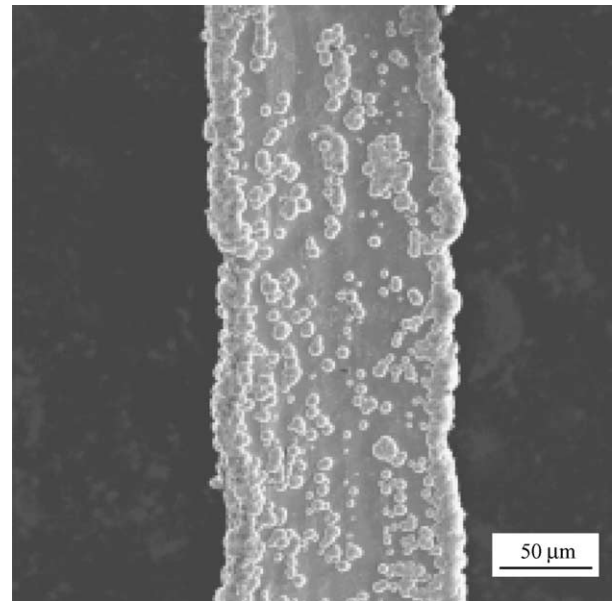


Fig. 3. Scanning electron micrograph of a fibre, after electroplating with copper.

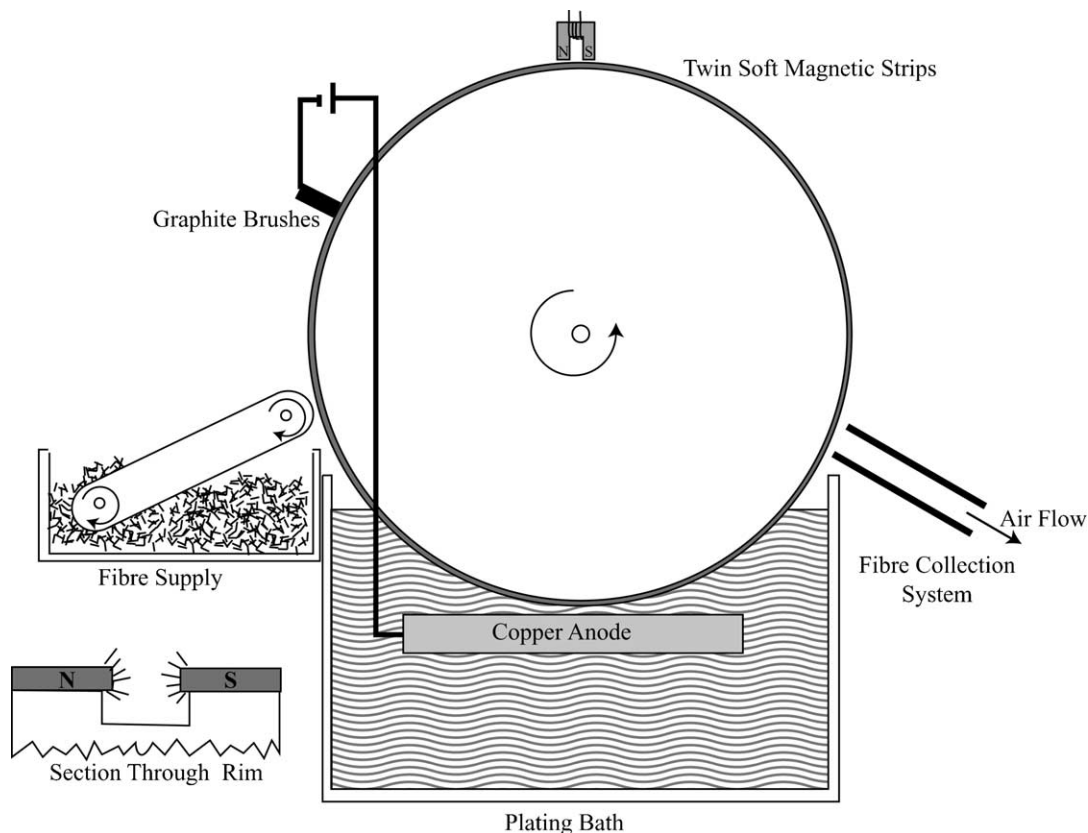


Fig. 2. Schematic depiction of the electroplating bath and the delivery and collection systems for short magnetic fibres.

testing machine and, prior to testing, cuts were made from each side to the central cut-out. The cross-head displacement was measured using an LVDT. All tests were conducted in displacement control at a rate of 0.1 mm min^{-1} . Fibres were tested in the as-received (melt spun) condition, and also after deposition of a $5 \mu\text{m}$ copper coating, with and without a subsequent heat treatment similar to that to which the short fibres were subjected during the sintering process.

2.3. Mechanical testing of the porous material

After the porous material had been extracted from the ampoule, it was prepared for tensile testing by infiltrating lengths of about 10 mm at each end with epoxy resin. The gauge length was thus about 10 mm. After

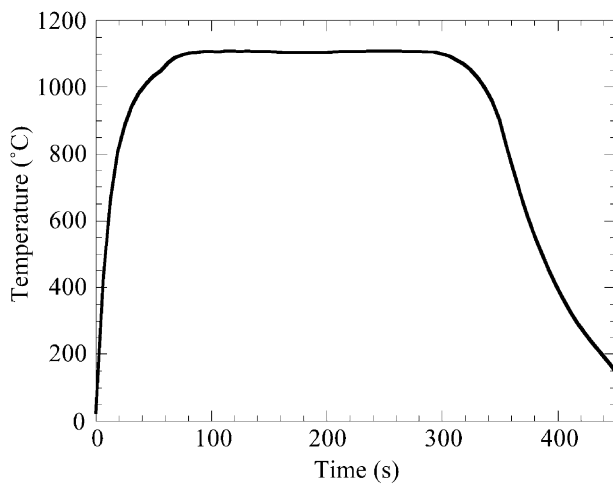


Fig. 4. Thermal history during sintering treatment.

the resin had set, these infiltrated sections were held in the grips and testing was carried out using the same machine and testing procedure as for the single fibre tests.

3. Results

3.1. Single fibre tensile strength and ductility

Typical stress–strain curves for as-received, as-coated and coated plus heat treated fibres are shown in Fig. 6. It can be seen that the presence of the coating reduces the ductility appreciably and also impairs the strength slightly. Observation of the coated fibres at higher magnification (Fig. 7) revealed the presence of a network of cracks around the copper deposits. This is probably due to hydrogen uptake during copper electro-deposition. This effect can be countered by a suitable low temperature heat treatment [12,13], and also by controlling hydrogen evolution by adjusting the plating process parameters and the plating bath composition. It can also be seen in Fig. 6 that the brief sintering heat treatment has induced a further reduction in ductility and strength. This may be attributed to chromium depletion adjacent to precipitated chromium carbide particles. Again, it may be possible to reduce this effect by heating to $700\text{--}950 \text{ }^\circ\text{C}$ to allow chromium to diffuse to the depleted areas [14]. Furthermore, the work hardening rate of the sintered material is noticeably lower than that of the other two types of specimen. This may be attributable to a reduction in dislocation density, and possibly to some slight microstructural coarsening, which occurred during the heat treatment. The nominal

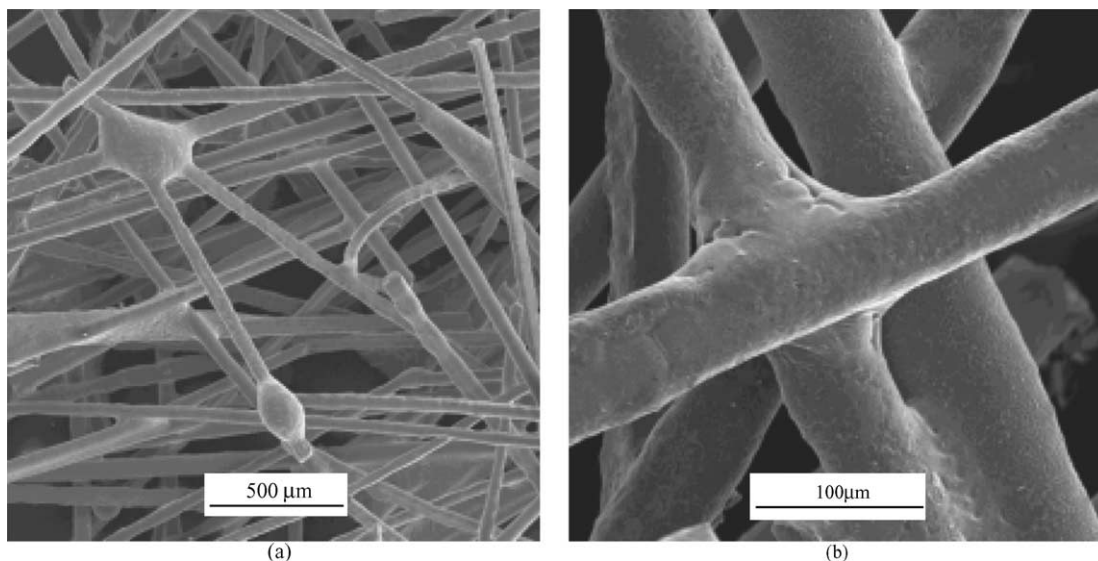


Fig. 5. Scanning electron micrographs of the sintered material, showing (a) the overall structure and (b) a high magnification view of a single fibre–fibre joint.

“work of fracture”, U , for a single fibre, measured as the area under the load-strain curve, is approximately 0.2 J m^{-1} for the coated/heat treated fibres.

3.2. Mechanical properties of the porous material

A typical stress–strain curve obtained during tensile testing of the porous material is shown in Fig. 8. It can be seen that the tensile strength is of the order of 1 MPa. There are very few data with which this can be compared. Ducheyne et al. [5] reported considerably higher strength values for their sintered fibre materials, but the

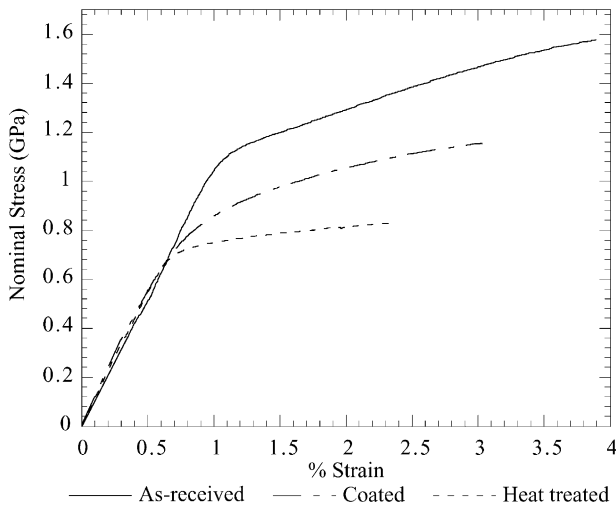


Fig. 6. Typical single fibre tensile testing data for as-received, coated and coated/heat treated fibres.

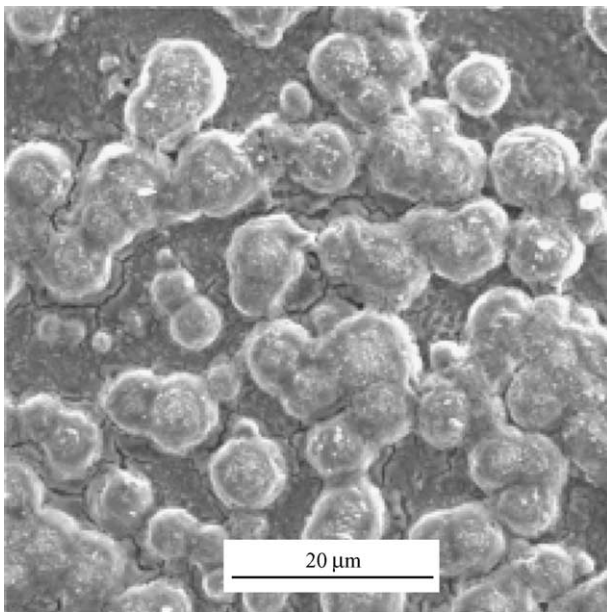


Fig. 7. Scanning electron micrograph of a coated fibre showing a network of cracks around copper deposits.

porosity levels were much lower and no meaningful comparison is possible. There have been some reports [1,4] of aluminium-based foams exhibiting similar, and even slightly higher, values, but these are usually for closed cell foams with rather lower porosity levels. Also, it is clear that most metallic foams are much more brittle than the material produced here. Depending on the manufacturing method employed, the low tensile strengths of metallic foams are commonly attributable to their brittle nature, often at least partly a consequence of the presence of ceramic particles or oxide films in the cell walls [4], or to the presence of weak necks or joints, which fail readily as stress becomes concentrated at them.

Material of the type being investigated here clearly has the potential for relatively high strength and toughness. This is apparent from the SEM micrographs shown in Fig. 9, which illustrate the high resistance to fracture exhibited by many of the fibre–fibre joints. Prediction of the maximum attainable strength for such material, based on the single fibre strength, is a little difficult. It might be imagined that a value of the order of the single fibre strength multiplied by the fibre volume fraction, and then further reduced by a factor of the order of 3 to account for the 3-D random fibre orientation distribution, could be appropriate. This would suggest a maximum strength of the order of 30 MPa in the present case. However, even if no joints fracture, and no fibres are damaged, this takes no account of stress concentration effects, which in a disordered material of this type are likely to cause some fibres to become highly stressed and fail prematurely, leading to an increase in the load borne by neighbouring fibres. Nevertheless, it might be useful to take the above figure as an absolute upper bound on the strength.

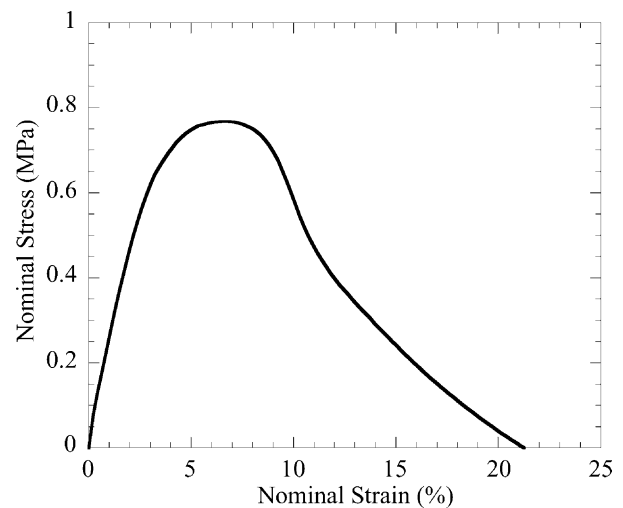


Fig. 8. Typical stress–strain plot for tensile testing of the porous material.

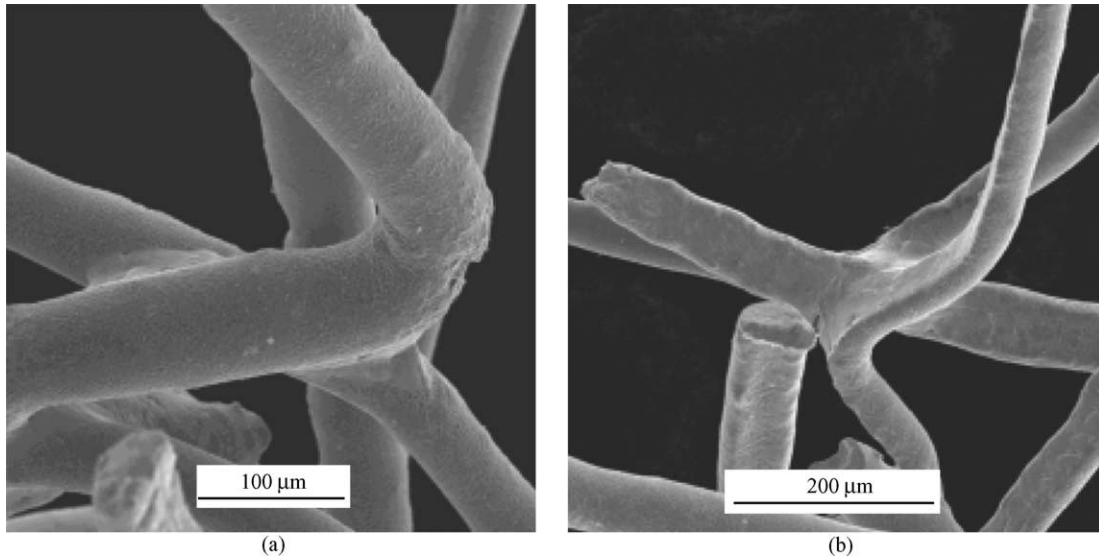


Fig. 9. Scanning electron micrographs showing fibre damage and fracture.

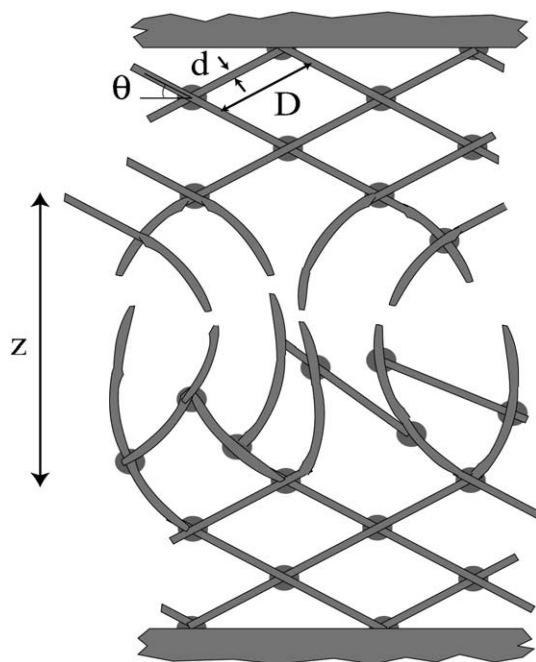


Fig. 10. Schematic depiction of the model [8,15] used for prediction of energy absorption during fibre deformation and fracture.

It is also possible to make an estimate of the expected fracture energy for this type of fibrous material. A previously-developed model [8,15] for deformation and rupture of a sintered fibre array of this type, based on the physical model depicted in Fig. 10, led to the following expression for the fracture energy (in $J m^{-2}$)

$$G = \left[\frac{4f \sin \theta}{\pi d^2} \right] U z \tag{1}$$

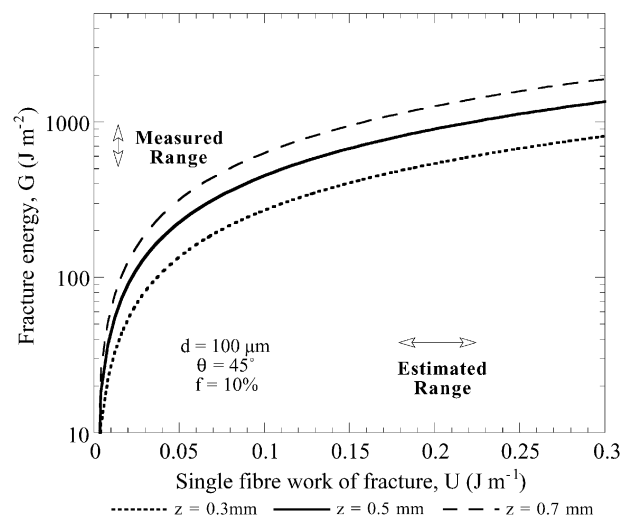


Fig. 11. Predicted fracture energy of the porous material, as a function of the single fibre work of fracture, according to Eq. (1). An indication is also given of the ranges of experimental values obtained for these two parameters.

in which f is the fibre volume fraction, θ is the average angle at which fibres are inclined (relative to the transverse direction), d is the fibre diameter, U is the single fibre “work of fracture” (in $J m^{-1}$) and z is the length of a deformation zone adjacent to the fracture plane, within which the fibres undergo substantial plastic deformation. The nominal fracture energy can be estimated as the area under a plot of nominal stress against displacement, which can be inferred from Fig. 8 to give a value of the order of $800 J m^{-2}$, since the gauge length was about 10 mm. A comparison with predictions obtained using Eq. (1) are shown in Fig. 11. It can be seen that the experimentally-estimated value of G

broadly agrees with model predictions (assuming a single fibre work of fracture of about 0.2 J m^{-1} —see above) if the deformation zone is taken to have a length of the order of 0.5 mm. This is consistent with the SEM observations. It might also be noted that this is the approximate spacing between the fibre–fibre joints in this material. The geometrical model illustrated in Fig. 10 leads to the following expression for the joint spacing:

$$D = \frac{d}{2} \left[\frac{\pi}{f \sin \theta \cos^2 \theta} \right]^{\frac{1}{2}} \quad (2)$$

which, on substitution of $d = 100 \text{ }\mu\text{m}$, $f = 0.1$ and $\theta = 45^\circ$, gives a value of about $500 \text{ }\mu\text{m}$. It might be expected that extensive fibre deformation would be confined to a region with a length of the order of the inter-joint spacing.

4. Conclusions

The following conclusions can be drawn from this work.

1. A procedure has been outlined for the production of highly porous, permeable metallic material, by liquid phase sintering of short stainless steel fibres, after electroplating them with copper. A novel method has been outlined for uniformly exposing short magnetic fibres to the electrolyte during electroplating. The process is quick, simple and amenable to large scale production.
2. The sintering process, which is completed in a few minutes at relatively low temperature, generates strong inter-fibre joints. During mechanical loading of the material, fibre fracture occurs preferentially to joint rupture.
3. Material produced in this way is relatively tough, considering that it is highly porous. A fracture energy value of the order of 1 kJ m^{-2} was obtained, using a simple method based on analysis of a tensile stress-displacement plot. This is consistent with predictions based on the assumption that this energy is primarily associated with plastic deformation of individual fibres within a process zone neighbouring the fracture plane, with no little or no failure of the joints. The width of this zone is apparently of the same order as the inter-joint spacing, as expected.

Acknowledgements

Support has been provided for AEM and AC via the Cambridge-MIT Institute (CMI) and for VG by the EPSRC. The authors are very grateful to Fibretech, and particularly to Lee Marston and Peter Rooney, for extensive collaboration and cooperation.

References

- [1] Gibson LJ. Properties and applications of metallic foams. In: Kelly A, Zweben C, Clyne TW, editors. *Comprehensive composite materials*. Amsterdam: Elsevier; 2000. p. 821–32.
- [2] Banhart J. Manufacture, characterisation and application of cellular metals and metalfoams. *Progress Mater Sci* 2001;46:559–632.
- [3] Gibson LJ. Mechanical behaviour of metallic foams. *Ann Rev Mater Sci* 2000;30:191–227.
- [4] Markaki AE, Clyne TW. The effect of cell wall microstructure on the deformation and fracture of aluminium-based foams. *Acta Mater* 2001;49(9):1677–86.
- [5] Ducheyne P, Aernoudt E, De Meester P. The mechanical behaviour of porous austenitic stainless steel fibre structures. *J Mater Sci* 1978;13:2650–8.
- [6] Ducheyne P, De Meester P, Aernoudt E. Isostatically compacted metal fibre porous coatings for bone ingrowth. *Powder Metallurgy International* 1979;11(3):115–9.
- [7] Delannay F, Clyne TW. Elastic properties of cellular metals processed by sintering mats of fibres (Paper presented at the Met-Foam 1999, Bremen, Germany, 14–16 June) p.293–298.
- [8] Markaki AE, Clyne TW. Mechanics of thin ultra-light stainless steel sandwich sheet material: part I- stiffness. *Acta Mater* 2003; 51(5):1341–50.
- [9] Gustavsson R. Formable sandwich construction material and use of the material as construction material in vehicles, refrigerators, boats etc, patent WO 98/01295, 15 January 1998, AB Volvo, International.
- [10] Markaki AE, Clyne TW. Ultra light stainless steel sheet material, US patent 10/000117, filed 31 October 2001, Cambridge University, UK.
- [11] Clyne TW, Gergely V. Processes of surface treating or coating fibres, UK patent, filed 13 February 2003, Cambridge University, UK.
- [12] Hydrogen embrittlement relief (baking) of steel parts. *Aerospace Material Specification AMS 2759/9*, Warrendale, Pa: SAE International.
- [13] Copper plating. *Aerospace Material Specification AMS 2418F*, Warrendale, Pa: SAE International.
- [14] Vander Voort GF, James HM. *ASM, Metals handbook, Vol. 9: metallography and microstructures*. OH, USA: American Society of Metals; 1985.
- [15] Markaki AE, Clyne TW. Mechanics of thin ultra-light stainless steel sandwich sheet material: part II-resistance to delamination. *Acta Mater* 2003;51(5):1351–7.